



Acute Inflammation Confers Enhanced Protection against *Mycobacterium tuberculosis* Infection in Mice

Tucker J. Piergallini,^{a,b} Julia M. Scordo,^{a,c} Paula A. Pino,^d Larry S. Schlesinger,^a Jordi B. Torrelles,^d Joanne Turner^a

^aHost-Pathogen Interactions Program, Texas Biomedical Research Institute, San Antonio, Texas, USA

^bBiomedical Sciences Graduate Program, The Ohio State University, Columbus, Ohio, USA

^cThe Barshop Institute, The University of Texas Health Science Center at San Antonio, San Antonio, Texas, USA

^dPopulation Health Program, Texas Biomedical Research Institute, San Antonio, Texas, USA

ABSTRACT Inflammation plays a crucial role in the control of *Mycobacterium tuberculosis* infection. In this study, we demonstrate that an inflammatory pulmonary environment at the time of infection mediated by lipopolysaccharide treatment in mice confers enhanced protection against *M. tuberculosis* for up to 6 months postinfection. This early and transient inflammatory environment was associated with a neutrophil and CD11b⁺ cell influx and increased inflammatory cytokines. *In vitro* infection demonstrated that neutrophils from lipopolysaccharide-treated mice exhibited increased association with *M. tuberculosis* and had a greater innate capacity for killing *M. tuberculosis*. Finally, partial depletion of neutrophils in lipopolysaccharide-treated mice showed an increase in *M. tuberculosis* burden, suggesting neutrophils played a part in the protection observed in lipopolysaccharide-treated mice. These results indicate a positive role for an inflammatory environment in the initial stages of *M. tuberculosis* infection and suggest that acute inflammation at the time of *M. tuberculosis* infection can positively alter disease outcome.

IMPORTANCE *Mycobacterium tuberculosis*, the causative agent of tuberculosis disease, is estimated to infect one-fourth of the world's population and is one of the leading causes of death due to an infectious disease worldwide. The high-level variability in tuberculosis disease responses in the human populace may be linked to immune processes related to inflammation. In many cases, inflammation appears to exacerbate tuberculosis responses; however, some evidence suggests inflammatory processes improve control of *M. tuberculosis* infection. Here, we show an acute inflammatory stimulus in mice provides protection against *M. tuberculosis* for up to 6 months, suggesting acute inflammation can positively affect *M. tuberculosis* infection outcome.

KEYWORDS *Mycobacterium tuberculosis*, inflammation, neutrophils, lipopolysaccharide, LPS

Tuberculosis (TB) disease, caused by the bacterium *Mycobacterium tuberculosis*, is a global health burden. In 2019, 1.4 million people died from TB, making TB the leading cause of death due to an infectious disease worldwide in that year (1). There is variability in *M. tuberculosis* infection outcomes among individuals, with some maintaining infection in a latent state (*M. tuberculosis* latency) and others developing active TB disease (1). Although individual responses to TB in humans and animal models have been characterized in many studies, the exact reasons why one host will respond differently from another is unknown.

Worse TB outcomes are associated with significant amounts of overall inflammation and host-directed damage (2), indicating that inflammation on its own may exacerbate *M. tuberculosis* infection. However, numerous studies have indicated the need for basic

Citation Piergallini TJ, Scordo JM, Pino PA, Schlesinger LS, Torrelles JB, Turner J. 2021. Acute inflammation confers enhanced protection against *Mycobacterium tuberculosis* infection in mice. *Microbiol Spectr* 9:e00016-21. <https://doi.org/10.1128/Spectrum.00016-21>.

Editor Christopher N. LaRock, Emory University School of Medicine

Copyright © 2021 Piergallini et al. This is an open-access article distributed under the terms of the [Creative Commons Attribution 4.0 International license](https://creativecommons.org/licenses/by/4.0/).

Address correspondence to Joanne Turner, joanneturner@txbiomed.org.

Received 13 April 2021

Accepted 2 June 2021

Published 7 July 2021

inflammatory processes in the control of TB disease, and others have shown enhanced inflammation can increase *M. tuberculosis* protection in various *in vitro* and *in vivo* models (3–11). Therefore, the role of inflammation in TB disease is not resolved. Comorbidities associated with increased TB susceptibility in humans are also associated with increased inflammation. HIV infection, while primarily conferring susceptibility to TB via depletion of CD4 T cells, is also associated with an increase in the overall inflammatory state (12–14). Diabetes increases active TB risk and itself is associated with systemically increased inflammation (15, 16). Chronic obstructive pulmonary disease (COPD) and smoking also are risk factors for TB and are also associated with inflammation (17–19). Another TB comorbidity, natural aging, can predispose individuals to reactivation of latent *M. tuberculosis* infection as well as increase TB disease mortality (20) and is associated with an increased pulmonary and systemic inflammatory state known as inflammaging (21–23). However, aged mice show an early control of *M. tuberculosis* infection associated with cellular inflammation, and while this is only transient, it does suggest that enhanced inflammation early helps control *M. tuberculosis* infection (8–11, 24). Other studies have also indicated enhanced inflammation and cytokine secretion can improve mycobacterial control (3–11). Additionally, the observation that some individuals may be capable of early clearance of TB suggests that a robust early inflammatory response can mediate control of *M. tuberculosis* or at least an alteration in how latent *M. tuberculosis* infection is established (25, 26). How inflammation can protect or worsen TB disease in these highly variably disease states and models is unknown and warrants further study to better understand the variable outcomes of TB.

To determine how acute inflammation can influence *M. tuberculosis* infection outcome, we utilized short-term low-dose lipopolysaccharide (LPS) treatment in mice to generate an increased acute systemic and pulmonary inflammatory response at the time of *M. tuberculosis* infection. LPS treatment caused an increase of inflammatory cytokines and myeloid cells, primarily neutrophils and CD11b⁺ cells, in the mouse lungs. Following *M. tuberculosis* infection, LPS-treated mice had a significant reduction of *M. tuberculosis* burden evident as early as 7 days postinfection, an effect that persisted for at least 6 months. *In vitro* analyses suggested neutrophils play a role in early *M. tuberculosis* control through *in vivo* depletion of neutrophils in LPS-treated mice prior to *M. tuberculosis* infection, although the contribution of other immune cells in the lung cannot be ruled out. Our findings confirm that a transient, acute, increased inflammatory environment at the time of *M. tuberculosis* entry into the lung can impact the course of infection by reducing *M. tuberculosis* burden in the lung, adding further information to discern why *M. tuberculosis*-exposed people have different infection and disease outcomes.

RESULTS

LPS causes pulmonary and systemically increased inflammation in mice. To evaluate the impact of acute inflammation on *M. tuberculosis* infection, we injected male BALB/c mice with LPS or saline via the intraperitoneal (i.p.) route every 24 h, for 4 total injections (Fig. 1A). Two hours after the fourth injection, termed day 0, we analyzed the local inflammatory response in the lungs. Tumor necrosis factor (TNF), interleukin-1beta (IL-1 β), IL-6, IL-12p70, and IL-10 were significantly increased in the lungs of LPS-injected mice (LPS mice) (Fig. 1B). We also saw a concomitant increase of TNF, IL-1 β , IL-6, and IL-10 in the spleens of LPS mice, while IL-12p70 showed no differences (see Fig. S1A in the supplemental material). C-reactive protein (CRP) levels showed no difference in the lung (Fig. S1B) but was increased in spleen and liver (Fig. S1B). To confirm LPS affected different mouse sexes and strains the same, we injected female BALB/c and male C57BL/6 mice with LPS and saw the same increase in lung inflammation as that observed in male BALB/c mice, with the exception that IL-12p70 was not increased in male C57BL/6 lungs (Fig. S1C and D).

Acute inflammation protects mice from *M. tuberculosis* infection. We infected male BALB/c LPS mice with *M. tuberculosis* on day 0 (4 days after initiation of LPS/saline treatment), injected with LPS/saline daily for 2 more days, and rested until the indicated time points (Fig. 1A). At 1 day postinfection (dpi), we found no difference in CFU

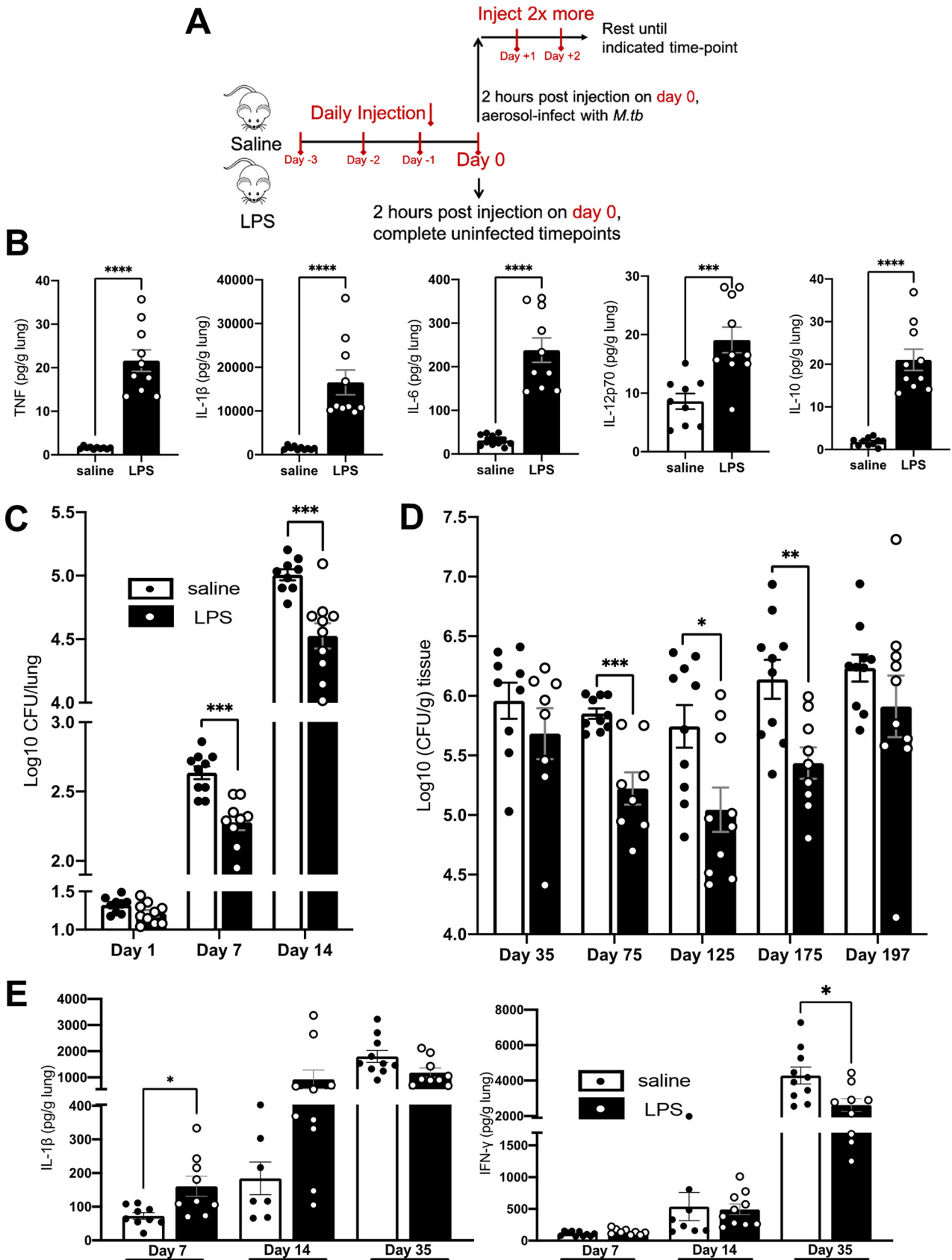


FIG 1 Cytokines and CFU in LPS mice. (A) Schematic of injection scheme. (B) Male BALB/c mice were injected with LPS as described in the text. On day 0, lungs were isolated and protein content determined via Luminex, normalized to organ mass. Protein levels of TNF, IL-1 β , IL-6, IL-12p70, (Continued on next page)

numbers (Fig. 1C), whereas at 7 and 14 dpi we saw significantly fewer CFU ($\sim 0.5 \log_{10}$) in LPS mice (Fig. 1C). To determine if the early control of *M. tuberculosis* was sex or mouse strain specific, we repeated these studies in female BALB/c mice and male C57BL/6 mice, showing that at 14 dpi, female BALB/c and male C57BL/6 LPS mice also had significantly fewer CFU than saline-injected mice (saline mice) (Fig. S2A and B). These results suggest that the effects of LPS on the early control of *M. tuberculosis* was not sex or strain specific but was related to LPS-induced inflammation. We further determined the CFU content at 35, 75, 125, 175, and 197 dpi and observed lower CFU levels (~ 0.25 , ~ 0.6 , ~ 1.0 , ~ 1.0 , $\sim 0.4 \log_{10}$ [CFU/g tissue], respectively) in LPS mice at all time points (Fig. 1D), although only days 75, 125, and 175 showed statistical significance.

When determining cytokine protein levels at 7, 14, and 35 dpi, we observed that IL-1 β levels in the lung were elevated at 7 dpi, with a trend increase at 14 dpi (Fig. 1E). Gamma interferon (IFN- γ) levels in lung showed no differences at 7 and 14 dpi (Fig. 1E). TNF levels showed no differences at 7 dpi but showed a trend increase at 14 dpi compared to saline (Fig. S2C). At 35 dpi, LPS mouse lungs showed significantly less IFN- γ and a decrease of IL-1 β and TNF, likely a result of their lower level of *M. tuberculosis* CFU burden at this time compared to saline-treated *M. tuberculosis*-infected mice (Fig. 1E and Fig. S2C).

LPS mice have more activated myeloid cells in the lungs. To determine the cellular mechanism behind the early *M. tuberculosis* control in LPS mice, we analyzed lung cellular profiles at day 0, prior to infection. LPS mice had more total cells (Fig. 2A), more total viable cells (Fig. 2B), and more myeloid cells (CD45⁺ SSC^{hi}) per lung (Fig. 2C). We used side scatter screening to obtain an estimate of myeloid cells in the lung, but contamination of other cell types in this specific population cannot be fully ruled out (27). Flow gating schemes and representative images of LPS- or saline-treated mouse profiles are shown in Fig. S3. Further analysis showed that LPS mice had larger amounts of neutrophils (CD11b⁺ Ly6G^{hi}) (Fig. 2D), alveolar macrophages (AMs) (Ly6G^{lo/neg} CD11c⁺ SiglecF⁺) (Fig. 2E), and cells that both singularly expressed CD11b (Ly6G^{lo/neg} CD11b⁺ CD11c⁻) (Fig. 2F) and dually expressed CD11b and CD11c (Ly6G^{lo/neg} CD11b⁺ CD11c⁺) (Fig. 2G) in LPS mice. Eosinophil (eos.) (Ly6G^{lo/neg} CD11c⁻ SiglecF⁺) numbers were relatively unchanged (Fig. 2H). Regarding CD11b⁺ cells, our hierarchical gating scheme attempted to identify cells of monocyte origin and macrophages, but as these cells lacked further characterization, we subsequently refer to these cells as CD11b⁺ cells. CD80 is upregulated on macrophages after activation (28), and we found higher numbers of CD80⁺ CD11b⁺ CD11c⁻ cells and CD80⁺ CD11b⁺ CD11c⁺ cells (Fig. 2I and J) in LPS mice. No differences were seen in CD80⁺ AMs (Fig. 2K). We also determined CD11b expression on neutrophils and CD11b⁺ CD11c⁻ cells and found a significantly lower level of CD11b mean fluorescence intensity (MFI) on neutrophils and a significantly higher CD11b MFI on CD11b⁺ cells (Fig. 2L and M) in LPS mice, suggesting higher CD11b surface expression on the CD11b⁺ cells and less on neutrophils from LPS mice.

Elevated numbers of myeloid cells in LPS mice persist at 1 week but normalize by 2 weeks after *M. tuberculosis* infection. We next determined when, and if, the levels of myeloid cells normalized in *M. tuberculosis*-infected LPS mice relative to *M. tuberculosis*-infected saline mice. Total number of cells showed no differences in *M. tuberculosis*-infected LPS mice at 7 and 14 dpi (Fig. 3A). Total numbers of viable cells, however, were elevated at 7 dpi, but no differences were seen between groups at 14 dpi (Fig. 3B). The same trend was observed in total myeloid cells at 7 and 14 dpi (Fig. 3C). Flow cytometric analysis of specific myeloid cell populations showed higher numbers of neutrophils (Fig. 3D), CD11b⁺ CD11c⁻ cells (Fig. 3E), and CD11b⁺ CD11c⁺ cells (Fig. 3F) in *M. tuberculosis*-infected LPS mice at 7 dpi, which normalized to *M.*

FIG 1 Legend (Continued)

and IL-10 are shown. (C and D) LPS or saline BALB/c mice were aerosol infected with *M. tuberculosis* as described in the text. CFU burdens at the indicated time point of whole (C) or partial (D) lungs from male (C) and female (D) mice are shown. Partial lung CFU numbers were normalized to lung mass. (E) At the indicated time point, protein levels via ELISA of IL-1 β and IFN- γ in male BALB/c mice are shown. Data are representative of 2 independent experiments of 4 or 5 mice in each group. Unpaired Student's *t* test, *, $P < 0.05$; **, $P < 0.01$; ***, $P < 0.001$; ****, $P < 0.0001$.

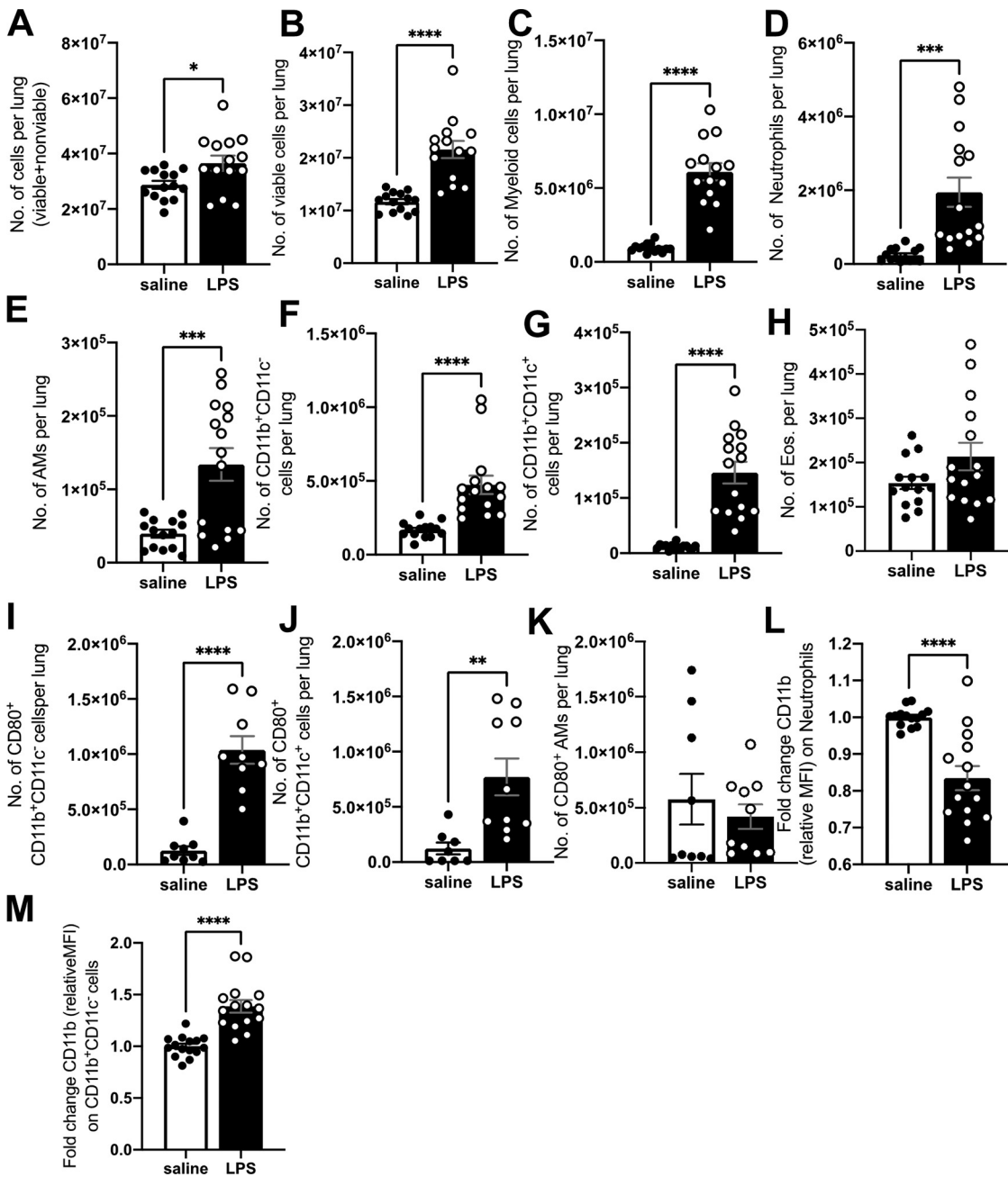


FIG 2 Day 0 lung cell profiles. Single-cell lung suspensions were obtained at day 0 (uninfected) from male BALB/c mice. (A and B) Total number of cells (viable+nonviable) (A) and total number of viable cells (B) per lung. (C to M) Flow cytometric analysis of single-cell suspensions. Gating was done as described in Fig. S3. (C to H) Number (No.) of myeloid cells ($CD45^+ SSC-L^{hi}$) (C), neutrophils ($CD11b^+Ly6G^+$) (D), alveolar macrophages (AMs) ($Ly6G^{lo/neg}CD11c^+SiglecF^+$) (E), $CD11b^+$ cells ($Ly6G^{lo/neg}CD11b^+CD11c^-$) (F), $CD11b^+CD11c^+$ cells ($Ly6G^{lo/neg}CD11b^+CD11c^+$) (G), and eosinophils (eos.) ($Ly6G^{lo/neg}CD11c^-SiglecF^+$) (H) per lung. Absolute numbers of cells per lung are shown. (I to K) No. of $CD80^+$ $CD11b^+CD11c^-$ cells (I), $CD80^+$ $CD11b^+CD11c^+$ cells (J), and $CD80^+$ AMs (K) per lung. (L to M) Relative fold change $CD11b$ expression (MFI) on neutrophils (L) and $CD11b^+$ cells (M) relative to saline. Data are representative of 2 to 3 independent experiments with 4 to 5 mice in each group. Unpaired Student's *t* test, *, $P < 0.05$; **, $P < 0.01$; ***, $P < 0.001$; ****, $P < 0.0001$.

tuberculosis-infected saline mice by 14 dpi. AMs (Fig. 3G) and eos. (Fig. 3H) showed no significant differences at 7 or 14 dpi. Elevated cell numbers in LPS mice compared to saline mice at 7 dpi, but not 14 dpi, indicated that the inflammatory stimulus from LPS treatment in *M. tuberculosis*-infected LPS mice was acute. Furthermore, we observed $CD11b$ MFI differences for both neutrophils and $CD11b^+CD11c^-$ cells at 7 dpi, but

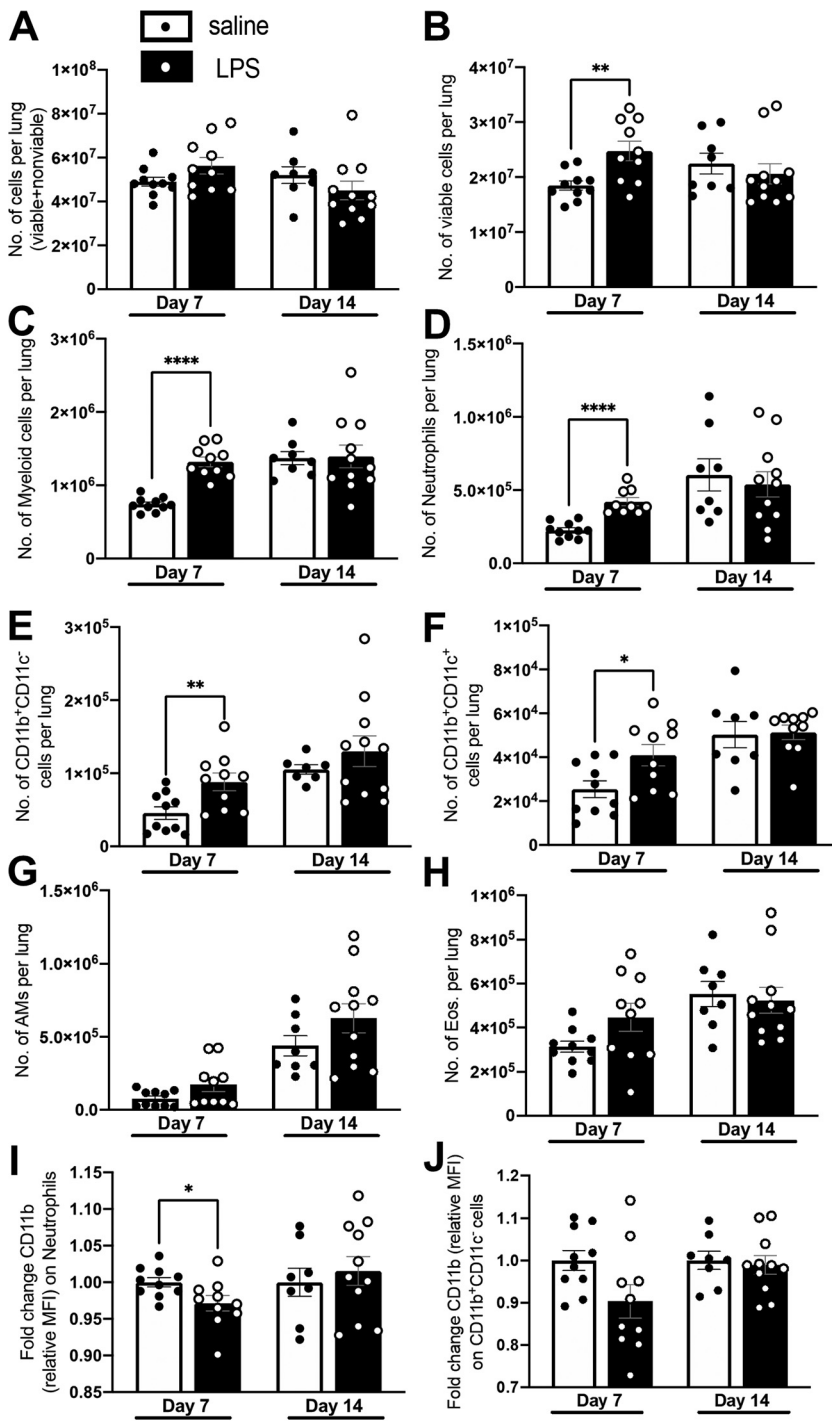


FIG 3 Lung cell profiles at 7 and 14 dpi. Lung single-cell suspensions prepared at the indicated time point postinfection as described from male and female BALB/c mice. (A and B) Total number of cells (viable+nonviable) (A) and total number of viable cells (B) per lung. (C to J) Flow cytometric analysis of single-cell suspensions. Gating was done as described in Fig. S3. (C to H) Number (No.) of myeloid cells (CD45⁺ SSC-L^{high}) (C), neutrophils (CD11b⁺ Ly6G⁺) (D), CD11b⁺ cells (Ly6G^{low/neg} CD11b⁺ CD11c⁻) (E), CD11b⁺ CD11c⁺ cells (Ly6G^{low/neg} CD11b⁺ CD11c⁺) (F), AMs (Ly6G^{low/neg} CD11c⁺ SiglecF⁺) (G), and eos. (Ly6G^{low/neg} CD11c⁻ SiglecF⁺) (H) per lung. (I to J) Relative fold change of CD11b expression (MFI) on neutrophils (I) and CD11b⁺ cells (J) relative to saline. Data are representative of 2 independent experiments with 4 to 5 mice in each group. Unpaired Student's *t* test, *, *P* < 0.05; **, *P* < 0.01; ****, *P* < 0.0001.

only the former was significant (Fig. 3I and J). At 14 dpi, CD11b MFI differences were normalized on neutrophils and CD11b⁺ CD11c⁻ cells from LPS and saline mice (Fig. 3I and J). These results show that the *M. tuberculosis*-infected LPS mice were under acute inflammation at the time of infection, and the cellular events responsible for the early protection against *M. tuberculosis* likely occurred within the first week postinfection. This was supported by the lower number of CFU in LPS mice as early as 7 dpi (Fig. 1C).

CD11b⁺ cells from LPS mice do not contribute to *in vitro* control of *M. tuberculosis*.

To determine the contribution of macrophages in the early *M. tuberculosis* control by LPS mice, we measured mRNA expression levels of several inflammatory transcription factors (CIITA, IRF1, and IRGM1) (29–32) from adherent lung cells at day 0 (uninfected) and 7 and 14 dpi. Flow cytometric analysis found the majority of adherent cells to be AMs, with some CD11b⁺ cells (total adherent cells, referred to as pulmonary macrophages) (~60% AMs, ~6% CD11b⁺ cell; Table S1). We observed no differences in CIITA mRNA levels at any time point (Fig. 4A), whereas IRF-1 and IRGM-1 showed an increase in *M. tuberculosis*-infected LPS mice at 7 dpi only (Fig. 4B and C). We concluded that pulmonary macrophages in LPS mice transiently upregulated inflammatory transcription factors after day 0.

We next purified CD11b⁺ cells at day 0 (uninfected) from LPS or saline mice based on CD11b positive magnetic selection (~94% CD11b⁺ cells; Table S1), infected *in vitro* with green fluorescent protein (GFP)-expressing *M. tuberculosis* Erdman, and determined CFU numbers at 2 h and 1, 2, 3, and 5 dpi. We observed no differences between groups at 2 h and 1 dpi, but 2, 3, and 5 dpi showed significantly higher *M. tuberculosis* CFU numbers in CD11b⁺ cells isolated from LPS mice (Fig. 4D). This suggested that the CD11b⁺ cell infiltrates we saw in LPS mouse lungs at day 0 do not contribute to the early control we see after *in vivo* infections and may be detrimental.

Neutrophils are responsible for enhanced control of *M. tuberculosis* infection in LPS mice. LPS treatment also increased neutrophils in the lung (Fig. 2D). To determine the potential involvement of neutrophils in control of *M. tuberculosis* infection in LPS mice, we isolated neutrophils via Ly6G positive magnetic selection at day 0 (uninfected) (~98% neutrophils; Table S1) and infected the purified cells *in vitro* with GFP-*M. tuberculosis* Erdman. At 30 min, 1 h, and 2 h postinfection, we determined CFU numbers (Fig. 5A). While at each time point there was no significant difference between CFU numbers in LPS and saline mice, we elected to analyze the differences between samples at the different time points by calculating the fold change of the 2-h CFU time point over the 30-min CFU time point among samples originating from the same mouse. We found a greater fold change of LPS neutrophil CFU numbers (2 h versus 30 min) than saline neutrophil CFU numbers (Fig. 5B), suggesting a greater magnitude of *M. tuberculosis* control in LPS neutrophils. When we analyzed the infection using single-blinded immunocytochemistry (ICC) microscopy (Fig. 5C), we found no differences in *M. tuberculosis* association with neutrophil extracellular traps (NETs), but the numbers of *M. tuberculosis* colocalizing with intact neutrophils was significantly increased in neutrophils from LPS mice compared to saline mice (Fig. 5D).

To confirm that LPS neutrophils were responsible for conferring increased control of *M. tuberculosis*, we partially depleted neutrophils over the course of *in vivo* infection (~50% depletion efficiency; Table 1). At 7 dpi, *M. tuberculosis*-infected LPS mice depleted of neutrophils showed higher levels of *M. tuberculosis* CFU (~0.25 log₁₀) than *M. tuberculosis*-infected LPS mice injected with the isotype control antibody (Fig. 6), although variability was seen, as some mice were observed with no CFU differences between the groups. Increased killing *in vitro* (Fig. 5), together with these results, suggests neutrophils were involved in the increased early control of *M. tuberculosis* infection in LPS mice *in vivo*, although the contribution of other cell types in this early control phenomenon cannot be ruled out.

DISCUSSION

Inflammation can affect the control of TB disease (33–35), yet the impact of basally increased inflammation (occurring in the elderly, persons with lung coinfections, those

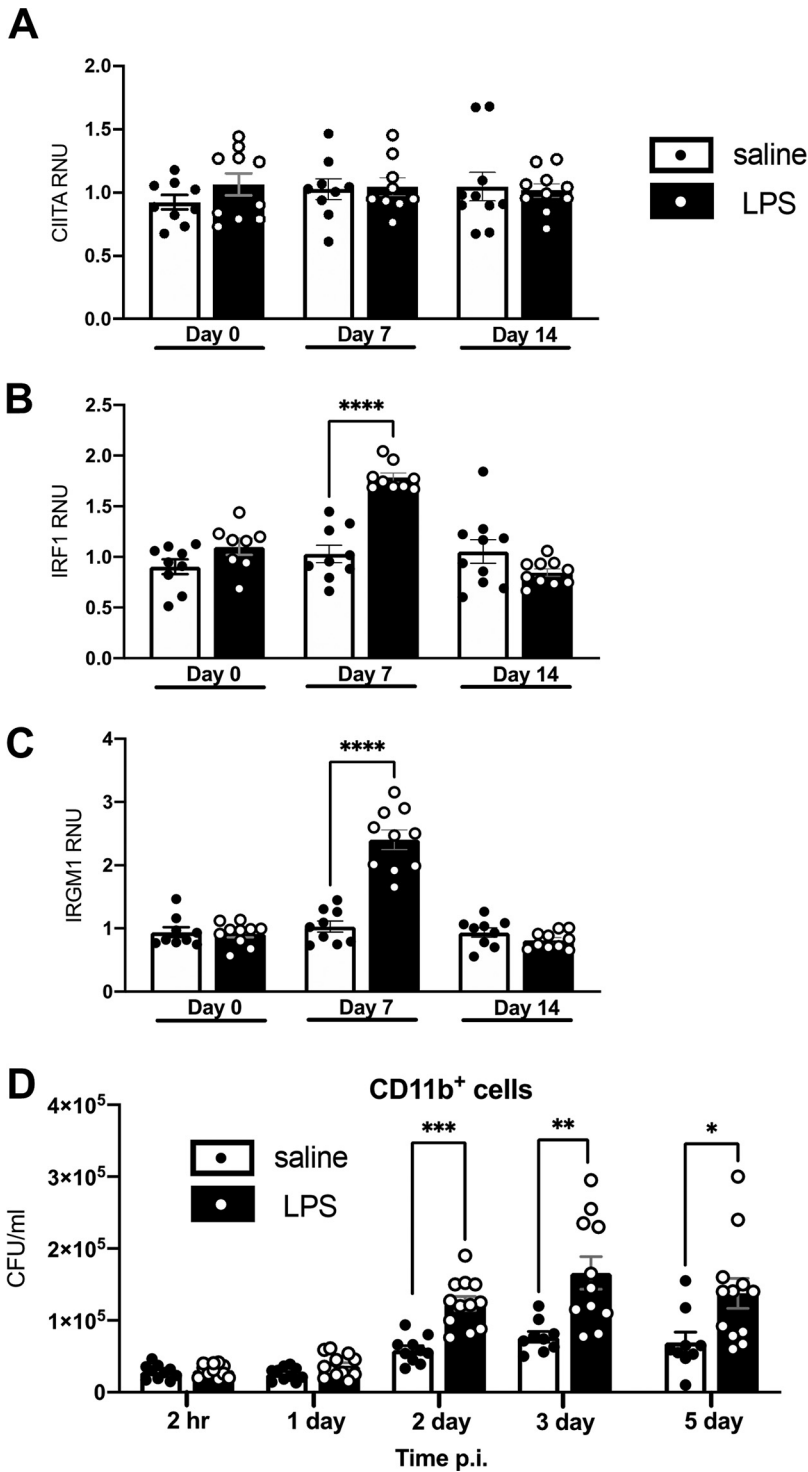


FIG 4 Lungs cells from LPS mice are transiently activated, while CD11b⁺ cells are detrimental to *in vitro* *M. tuberculosis* infection. (A to C) At the indicated time point, RNA was isolated from pulmonary macrophages from female BALB/c mice and quantified using quantitative real-time PCR. CIITA (A), IRF1 (B), and IRGM1 (C) levels are shown. Data are expressed as relative numerical units (RNU) relative to saline mice and is representative of 2 independent experiments of 4 or 5 mice in each group. (D) CD11b⁺ cells were isolated from uninfected female BALB/c mice and infected *in vitro* with *M. tuberculosis*. Numbers of CFU at the indicated time point are shown. Data are expressed as CFU/ml and are represented by 3 independent experiments with 2 to 5 samples in each group. Unpaired Student's *t* test, *, *P* < 0.05; **, *P* < 0.01; ***, *P* < 0.001; ****, *P* < 0.0001.

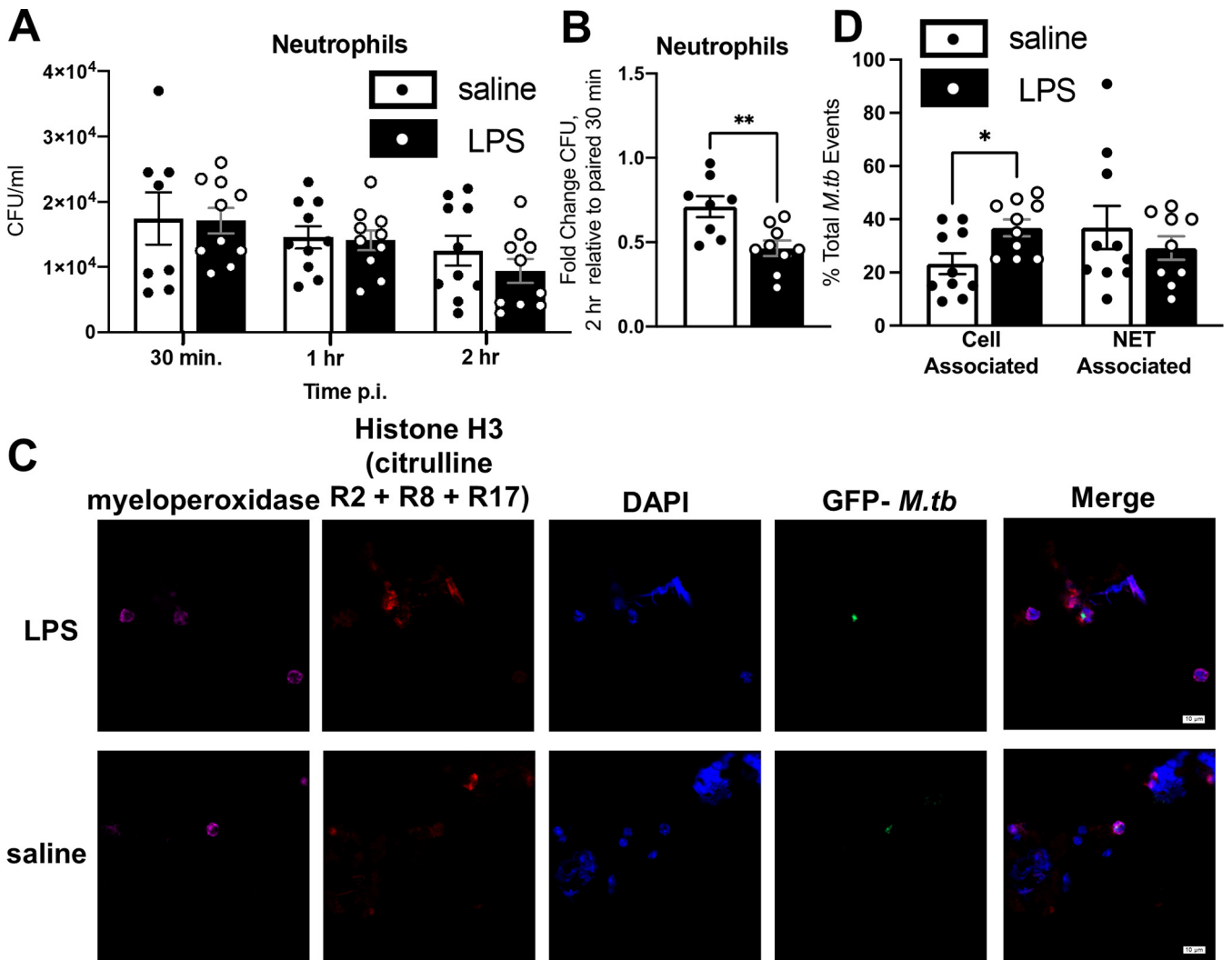


FIG 5 Neutrophils from LPS mice are capable of increased *M. tuberculosis* killing. Neutrophils were isolated from uninfected female BALB/c mice as described. (A) Number of CFU during *in vitro* infections. (B) Fold change of CFU numbers over 2 h of neutrophil infection, calculated relative to paired 30-min data. (C) Immunocytochemistry of neutrophil infections. Pink, myeloperoxidase; red, citrullinated histone H3 (R2+R8+R17); blue, DAPI; green, GFP *M. tuberculosis*. Representative images of a GFP-*M. tuberculosis* event colocalized with an intact cell (neutrophil) are shown. (D) The location of GFP-*M. tuberculosis* in each well, expressed as percentage of total *M. tuberculosis* events. Slides were analyzed in a single-blinded manner. Nineteen to 22 GFP-*M. tuberculosis* events were analyzed per well. Cell-associated, GFP-*M. tuberculosis* colocalized with an intact cell; NET associated, GFP-*M. tuberculosis* colocalized with a neutrophil NET. Data are representative of 2 independent experiments with 4 to 5 samples in each group. Unpaired Student's *t* test, *, $P < 0.05$; **, $P < 0.01$.

with environmental insult, etc.) at the time of *M. tuberculosis* infection has received limited attention (36–38). To investigate this, we developed a mouse model to test if acute inflammation induced by a short-term low-level LPS delivery could alter control of *M. tuberculosis* infection. LPS was chosen as a commonly used stimulus to induce acute inflammation in the mouse model (39–43), primarily signaling through toll-like receptor 4 (TLR4) to generate an inflammatory response (44). Although LPS signaling may not be representative of other inflammatory states generated by signaling through other TLRs and pathogen recognition receptors, it is a well-characterized acute inflammatory stimulus with predictable cytokine responses and a multitude of cellular activations and influxes (45–47). Mice injected with LPS established an acute pulmonary and systemic inflammatory state and an influx of neutrophils and CD11b⁺ cells into the lungs prior to infection, which can be expected after an acute inflammatory stimulus such as LPS (48). After *M. tuberculosis* infection, LPS mice had lower *M. tuberculosis* burden than controls as early as 7 dpi and continuing up to 6 months postinfection. *In vitro* and *in vivo* studies demonstrated that neutrophils were involved in the enhanced

TABLE 1 Neutrophils present in mice lungs depleted of neutrophils at day 0^a

Sample	No. of neutrophils \pm SD (if applicable)	Depletion efficiency versus LPS or saline isotype (%)	Fold change versus saline isotype
LPS isotype	7.08×10^6		32.32
LPS depletion	$3.58 \times 10^6 \pm 4.25 \times 10^5$	50.56	16.34
Saline isotype	2.19×10^5		1.00
Saline depletion	1.11×10^5	50.68	0.50

^aThe average absolute numbers of neutrophils per lung at day 0 are shown. Saline mice were included as a reference. Data are representative of 1 independent experiment with 1 to 2 samples in each group.

control of *M. tuberculosis* in LPS mice. These findings suggest that acute inflammation can confer protection against *M. tuberculosis* infection in the mouse model.

Our results suggest that an acute inflammatory state at the time of *M. tuberculosis* infection can be protective against *M. tuberculosis*. Examples of this in the literature include studies in old mice, which are chronically inflammatory, both in the periphery and the lung (49–51). This chronic inflammatory status makes old mice display an early control of *M. tuberculosis* infection compared to their younger counterparts (24, 52, 53). This early control is considered a consequence of the chronic but moderate inflammatory state at the time of infection in old mice, as work from our group has indicated (8–11), and we showed that innate cells in the lungs of old mice are preactivated and behave differently in response to *M. tuberculosis* (49). In contrast to LPS mice (acute model), old mice (chronic model) cannot sustain control, likely due to their reported reduced adaptive immune function (54, 55), and old mice succumb to the infection earlier than young mice (52, 56). Adaptive immune function was not investigated in LPS mice, but as we observed decreased *M. tuberculosis* burden in LPS mice up to 6 months p.i., the longest time point we tested, the initial innate response against *M. tuberculosis* in LPS mice was enough to maintain protection long term in our model. Beyond the initial decrease in bacterial burden, however, we do not know how LPS mice were able to maintain a lower level of *M. tuberculosis* long term. It may be due to alteration of the cellular profiles during long-term infection or by restructuring of lung granulomas. Alternatively, the neutrophil influx observed in LPS mice may activate other cells, such as dendritic cells, enhancing their actions to keep the *M. tuberculosis*

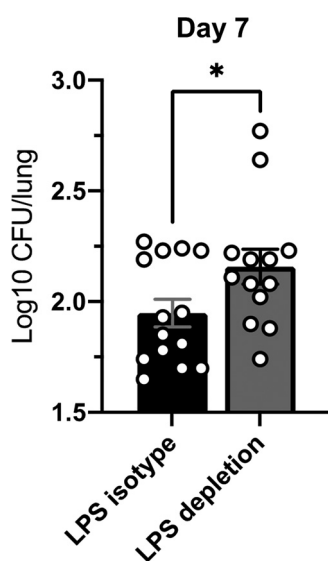


FIG 6 Neutrophils drive control in LPS mice. Neutrophils were depleted from LPS and saline female BALB/c mice using monoclonal antibodies against Ly6G as described in the text. Numbers of CFU at 7 dpi in LPS mice injected with depletion or isotype antibodies are shown. Data are representative of 4 independent experiments with 3 to 4 mice in each group. Unpaired Student's *t* test, *, $P < 0.05$.

level lower (57). The simplest explanation may be that LPS and saline mice, although given the same dose of *M. tuberculosis*, have a different bacterial burden at 14 dpi, the starting point when adaptive immunity against *M. tuberculosis* can first be detected in the lungs (58, 59), and this may be enough for LPS mice to maintain their bacterial burden using typical adaptive immunity. Resembling this effect, mice infected with different doses of *M. tuberculosis* show higher or lower levels of *M. tuberculosis* burden at late stages of the infection, depending on a higher or lower initial infectious dose, respectively (60, 61). It is interesting, though, that LPS mice do not lose their early control, either back to the level of saline mice, or show a worsening of burden. This implies their early inflammatory stimulus causes no negative long-term effects.

In human active TB, neutrophils are the most infected phagocytic cell and can provide a niche for *M. tuberculosis* persistence and survival (62). Furthermore, neutrophil influx to the lungs is associated with worse TB disease in patients (63). Neutrophils enter the lung in high numbers after *M. tuberculosis* infection, and are typically reported to kill *M. tuberculosis* via phagocytosis and subsequent killing as well as extracellular killing mechanisms (degranulation) (64, 65). Neutrophil NETs can also contribute to control via slowing of *M. tuberculosis* growth and *M. tuberculosis* death (66) but are also reported to contribute to the worsening of disease (67). The amount of conflicting information on neutrophils in *M. tuberculosis* infection suggests the role of neutrophils is context dependent. Indeed, rodent studies show that neutrophils play a beneficial role in early infection but a negative role at later stages (37, 38, 68, 69). A study of LPS-induced lung neutrophilia in rats showed reduced *M. tuberculosis* burden if LPS was delivered prior to infection, which was negated following neutrophil depletion (38). LPS delivery 10 days post-*M. tuberculosis* infection, however, had no effect. Our results from LPS mice corroborate these findings and suggest that neutrophils can play a beneficial role in early infection, if they are increased in number and primed prior to the arrival of *M. tuberculosis* to the lungs. In our own neutrophil depletion studies, however, we recognize that there was only a small increase ($\sim 0.25 \log_{10}$) of *M. tuberculosis* CFU numbers in LPS mice depleted of neutrophils compared to LPS mice with no neutrophil depletion. Additionally, some neutrophil-depleted LPS mice showed no difference in CFU at all. Complete depletion of neutrophils is challenging (66, 70–73) and we achieved 51% depletion in LPS mice, still representing a 16.34-fold increase in neutrophils compared to the basal levels seen in saline mice, which likely influenced the modest changes in CFU numbers. It is accepted that depletion of neutrophils in mice with the 1A8 clone is difficult for a variety of reasons (70). After depletion, the bone marrow generates neutrophils to maintain homeostasis (74), which, coupled with the LPS stimulus, likely caused abundant neutrophils present in the periphery to be depleted, resulting in incomplete depletion. Although we cannot conclude that neutrophils are the singular determinant of early control in LPS mice, we can speculate from their known involvement in inflammation (63, 75–77) that they contribute to the inflammation-mediated early control of *M. tuberculosis* infection in LPS mice.

The contribution of neutrophils in mediating some control of *M. tuberculosis* infection in LPS mice was supported by our *in vivo* flow cytometry data, where neutrophil numbers were increased most in lungs of LPS mice compared to other cells. Our *in vitro* work also suggested that neutrophils from LPS mice phagocytose and kill *M. tuberculosis* more effectively, although we observed differences in CFU numbers only after data pairing, possibly due to the low sensitivity of the CFU method. Infections with a multiplicity of infection (MOI) of 5:1 indicated that not all the bacteria were taken up by cells, possibly contributing to enumeration issues in this *in vitro* model. Additionally, during ICC experiments of neutrophils, we observed differences in *M. tuberculosis*-neutrophil colocalization between saline and LPS mice at 30 min of infection but no differences in CFU numbers during the 30 min time point itself. We believe this discrepancy results from the time difference between phagocytosis of the bacterium and its eventual killing (78). We suspect seeing early increases in colocalization of *M. tuberculosis* with LPS neutrophils sets up LPS neutrophils to show lower CFU numbers during the whole infection.

We observed less CD11b expression on LPS neutrophils, a component of complement receptor 3 (CR3) (79). CR3 is one of the major phagocytic receptors for *M. tuberculosis* and can be activated by *M. tuberculosis* on neutrophils, although it is not known if neutrophils directly use CR3 to phagocytose *M. tuberculosis* (79–81). Because we observed no negative impact in the colocalization of *M. tuberculosis* and LPS neutrophils, we can conclude that the lower levels of CD11b expression on LPS neutrophils had a limited effect. Interestingly, a recent experiment showed that lowering levels of CD11b expression on neutrophils resulted in increased protection against *M. tuberculosis* in a mouse model, although this was associated with decreased neutrophil accumulation in the lungs (82). Given the complicated and often disparate roles of neutrophils shown in the literature, more studies are needed to address the role of neutrophils in differing states of *M. tuberculosis* infection, especially in cases where neutrophil behavior is altered (37, 38, 68, 69, 82).

The other cell type we interrogated as potentially being responsible for control in LPS mice was CD11b⁺ cells. Our hierarchical flow cytometry gating scheme attempted to phenotype cells of monocyte origin (CD11b⁺ cells) (83); however, we were unable to specifically differentiate between monocytes, macrophages, and CD11b⁺-expressing dendritic cells. For simplicity, we labeled all cells in this gate CD11b⁺ cells, but they are likely of monocyte origin and make up a mixture of macrophages, monocytes, and dendritic cells (84). When we tested the cells *in vitro*, our results suggested CD11b⁺ cells were not major contributors to the increase in *M. tuberculosis* control seen LPS mice. As *M. tuberculosis* infections progress in a mouse, macrophages are known to be essential for infection control, and the transition of *M. tuberculosis* to interstitial macrophages has been shown to be beneficial (85, 86). However, interstitial macrophages can also provide *M. tuberculosis* a niche for survival (87–89). A recent experiment on an alveolar macrophage subset showing monocytic markers in old mice displayed worse control of *M. tuberculosis* (90), and in humans and mice infected with *M. tuberculosis*, a monocyte influx to the lungs correlates with worse TB disease outcome (91, 92). These findings substantiate the results from our *in vitro* infections of CD11b⁺ cells in LPS mice, where worse control of *M. tuberculosis* growth was seen *in vitro*. The exact consequence of the alterations in CD11b⁺ cells in LPS mice was not determined from the experiments we performed. However, it does signify inflammation can affect CD11b⁺ cell function, and we believe our work can be used as a starting point for future studies aimed at assessing the interplay between inflammatory CD11b⁺ cells/macrophages and *M. tuberculosis* in inflammatory disease states.

Overall, our results demonstrate that basal inflammation at the time of *M. tuberculosis* infection can positively impact infection outcome. We can conclude that neutrophils played a role in this early control but could not make a definitive conclusion whether CD11b⁺ cells were also directly involved in the early control of *M. tuberculosis* seen in our model, although our results do suggest that LPS causes changes in these cell types. In a broader sense, our results indicate that inflammation driven by acute insult at the time of *M. tuberculosis* infection can lead to improved long-term control of infection. In some states, inflammation may work to enhance protection against TB, but in a human host with other factors impacting the immune response (such as HIV coinfection, diabetes, COPD, etc.), these factors may override any positive benefits of inflammation, ultimately resulting in TB susceptibility. The results presented here with LPS mice may have relevance for other coinfections and disease states that cause a short-term (acute) pulmonary inflammation in the lung at the time of *M. tuberculosis* infection. In these cases, the initial bacterial burden may be lowered during early *M. tuberculosis* infection and maintained long term, giving rise to differential TB infection outcomes.

MATERIALS AND METHODS

Mice. Specific-pathogen-free male or female BALB/c and male C57BL/6 mice, 11 to 12 weeks old, were purchased from Charles River Laboratories (Wilmington, MA) or The Jackson Laboratory (Bar Harbor, ME). Male and female BALB/c mice were used as indicated in the figure legends. Mice were housed in animal biosafety level 2 (ABSL2) or ABSL3 facilities, in individually ventilated cages, and given sterilized water and standard chow *ad libitum*. Experimental and control mice were housed in separate cages and were acclimatized for at least 1 week before use in experiments. Mice were euthanized by

CO₂ asphyxiation. All procedures were approved by the Texas Biomedical Research Institute Institutional Laboratory Animal Care and Use Committee (IACUC), protocol number 1608 MU.

LPS mouse model. Lipopolysaccharides (LPS) (L3129-100MG; Sigma) were injected intraperitoneally (i.p.) with 20 μ g/mouse (BALB/c) or 50 μ g/mouse (C57BL/6) in 100 μ l normal saline (vehicle). Saline injections served as a control. The optimum LPS dose for each individual mouse strain to result in inflammation without persistent morbidity was determined, and mice were injected every 24 h \pm 2 h for 4 total injections. Experiments termed day 0 took place 2 h after the fourth injection. Alternatively, mice were infected with *M. tuberculosis* 2 to 4 h after the fourth injection, as described below. *M. tuberculosis*-infected mice were injected daily with LPS or saline for 2 more days for a total of 6 injections and rested until the indicated time point.

***M. tuberculosis* stocks.** *M. tuberculosis* Erdman (ATCC 35801) was obtained from the American Type Culture Collection (Manassas, VA). GFP-expressing *M. tuberculosis* Erdman was kindly provided by Horwitz and colleagues (93). Stocks were grown and delivered via aerosol as previously described (94). For *in vitro* infections, a frozen *M. tuberculosis* stock was plated onto 7H11 agar (Difco and BBL) supplemented with oleic acid-albumin-dextrose-catalase (OADC) enrichment and incubated for 11 to 13 days at 37°C. A *M. tuberculosis* single bacterial suspension was generated and diluted to working concentration as described previously (95).

***M. tuberculosis* aerosol infection and CFU number calculation.** Mice were exposed to a low-dose aerosol of *M. tuberculosis* Erdman using an inhalation exposure system (Glas-col) calibrated to deliver 10 to 30 CFU to the lungs of each mouse (96). Calculation of *M. tuberculosis* (CFU) burden at the indicated time points was performed by plating serial dilutions of whole or partial (superior, middle, inferior, and postcaudal lobes) lung homogenates onto OADC-supplemented 7H11 agar containing Mycobacteria Selectatab (Mast Group, UK). Plates were incubated at 37°C, and CFU were counted after 14 to 21 days and transformed to a log₁₀ scale. CFU counts obtained from partial lung homogenates were normalized to the mass of each partial lung.

Protein ELISA and Luminex analysis. Organ homogenates were thawed and the resulting supernatants analyzed for cytokines and proteins by enzyme-linked immunosorbent assay (ELISA) (BioLegend, BD, and R&D) and Luminex (R&D) according to the manufacturers' instructions. Protein levels were normalized to lung mass.

Lung cell isolation. As described previously, mice were euthanized and lungs perfused with 10 ml 1 \times Dulbecco's phosphate-buffered saline without calcium or magnesium (Gibco) (PBS) containing 50 U/ml heparin (Sigma) and placed into 2 ml complete Dulbecco's modified Eagle's medium (c-DMEM), DMEM (10-017-CV, Corning), 500 ml supplemented with filter-sterilized 5 ml HEPES buffer (1 M; Sigma), 10 ml MEM nonessential amino acid solution (100 \times ; Sigma), 5 ml penicillin-streptomycin (pen/strep) (100 \times ; Sigma), 660 μ l 2-mercaptoethanol (50 mM; Sigma), and 45 ml heat-inactivated fetal bovine serum (FBS) (Atlas Biologicals). A single-cell suspension was obtained using enzymatic digestion (49). Residual erythrocytes were lysed using Gey's solution (8 mM NH₄Cl, 5 mM KHCO₃ in water), passed through a 40- μ m strainer, and suspended in c-DMEM. The total number of viable cells was determined with acridine orange and propidium iodide (AO/PI) staining and counted on a Cellometer K2 cell counter (Nexcelom Bioscience).

Flow cytometry. Lung single-cell suspensions were washed once with 1 \times PBS and stained with Zombie Aqua fixable viability kit (1:100; BioLegend) for 15 min at room temperature (RT) in the dark. After incubation, cells were washed once with 1 \times PBS and incubated in TruStain FcX-Fc block (BioLegend) for 15 min at 4°C in the dark. Fc block was diluted in deficient RPMI (dRPMI; RPMI 1640 supplemented with HEPES and 1 g/liter sodium azide [ThermoFisher Scientific]) with 10% heat-inactivated FBS (dRPMI+FBS). Fc block was then removed and cells incubated in antibody cocktails (CD45.2, peridinin chlorophyll protein [PerCP]-cyanine5.5, clone 104; Ly6G, Alexa Fluor 488, clone 1A8; CD11b, allophycocyanin [APC]-cyanine7, clone M1/70; CD11c, APC, clone N418; Siglec-F, Brilliant Violet 421, clone S17007L; CD80, phycoerythrin [PE], clone 16-10A1; BioLegend) diluted in dRPMI+FBS for 20 min at 4°C in the dark. After staining, cells were washed once in dRPMI+FBS. For experiments completed at day 0 (uninfected mice), cells were fixed in 2% paraformaldehyde (PFA) for 15 min at RT in the dark and washed once more in dRPMI+FBS. For experiments completed after infection, cells were fixed in 4% PFA for 30 min at RT in the dark for ABLS3 removal and washed twice in dRPMI+FBS. All stained and fixed cells were suspended in dRPMI+FBS and stored at 4°C in the dark until data acquisition on a Beckman Coulter CyAn flow cytometer. Data analysis was performed using FlowJo v10 (BD Biosciences). Total numbers of specific cell populations per lung were calculated using the percentage of each population in the parent gate for absolute quantification multiplied by the total number of viable cells isolated from each sample.

Collection of adherent lung cells. Lung single-cell suspensions were incubated in tissue culture plates for 1 h at 37°C, 5% CO₂ (49). Plates were washed with c-DMEM to remove nonadherent cells. For RNA isolation, TRIzol (ThermoFisher Scientific) was added to the plates and vigorously pipetted. The TRIzol solution (containing adherent cell RNA) was frozen at -80° C until RNA extraction. For flow cytometric analysis, adherent cells were incubated in trypsin-EDTA (Sigma) for 15 min at 37°C, 5% CO₂, and c-DMEM was added to stop the reaction. Adherent cells were pooled and suspended in c-DMEM, and viable cell numbers were determined with AO/PI staining as described above. Flow cytometric analysis was performed as described above.

Real-time PCR. Frozen TRIzol samples were thawed, and RNA was extracted with chloroform, precipitated using isopropanol and 75% ethanol, and reconstituted in DNase/RNase-free water as previously described (49). cDNA was synthesized with random hexamers using an Omniscript RT kit (Qiagen). cDNA was quantified using TaqMan gene expression probes (ThermoFisher Scientific) and data collected using

an Applied Biosystems 7500 real-time PCR instrument. The $\Delta\Delta C_T$ method was used to quantify relative numerical units (RNU), normalized to endogenous 18S RNA, relative to saline.

Isolation of purified lung CD11b⁺ cells and neutrophil populations. Lung single-cell suspensions were prepared from noninfected mice as described above, with the exception that residual erythrocytes were not lysed with Gey's solution. For isolation of CD11b⁺ cells, lung suspensions from 2 saline-injected mice were pooled, whereas LPS lung suspensions were individually processed. As CD11b is also highly expressed on neutrophils and natural killer (NK) cells (97, 98), we developed a method that enriched lung single-cell suspensions for CD11b⁺ cells by depleting the suspensions of Ly6G⁺ cells (neutrophils) and CD49b⁺ cells (NK cells) via positive selection, followed by positive CD11b magnetic isolation to obtain the leftover cells. Briefly, suspensions were washed once with selection buffer (1 × PBS containing 2% FBS, 1 mM EDTA, and 1 × pen/strep), suspended at a concentration of 1 × 10⁸ viable cells/ml in 5 ml polypropylene tubes, and first depleted of neutrophils and NK cells using positive magnetic selection, with all incubations carried out in selection buffer using the MojoSort mouse Ly6G selection kit (BioLegend), the EasySep biotin positive selection kit II (Stemcell Technologies), and biotinylated anti-mouse CD49b antibody (25 μg/1 × 10⁸ viable cells; clone DX5; BioLegend) per each kits' instructions. Following Fc block incubation (Stem Cell), cells were incubated in Ly6G selection antibody and CD49b antibody together, followed by the Stem Cell selection cocktail. Finally, cells were incubated with Ly6G and Stem Cell selection magnetic beads together and selected out using magnets. From the resulting cell suspensions (depleted of neutrophils and NK cells), CD11b⁺ cells were isolated using positive magnetic selection using the EasySep mouse CD11b positive selection kit II (Stem Cell Technologies) according to the manufacturer's instructions. CD11b⁺ cell viability postisolation was 91.5% ± 1.5% (n = 10).

For isolation of lung neutrophils, single-cell suspensions were washed in selection medium and suspended at a concentration of 1 × 10⁸ viable cells/ml. Cells were incubated with normal rat serum (50 μl/1 × 10⁸ viable cells; Stem Cell Technologies and Jackson ImmunoResearch Laboratories) for 5 min at RT. Neutrophils were isolated using the MojoSort mouse Ly6G selection kit (BioLegend) according to the manufacturer's instructions. Neutrophil viability postisolation was 91.1% ± 4.2% (n = 10).

Purified CD11b⁺ cell or neutrophil suspensions were washed and suspended in 100 to 200 μl c-DMEM, and total viable cell numbers were determined with AO/PI staining. Cells were washed with 10 ml antibiotic-free c-DMEM (ABFc-DMEM; c-DMEM without pen/strep added) and suspended at a final concentration of 50,000 viable cells/150 μl in ABFc-DMEM.

In vitro M. tuberculosis infection of CD11b⁺ cells and neutrophils and CFU number determination.

Ninety-six-well plates and 8-well chamber slides were coated with poly-D-lysine (0.1 mg/ml; Gibco) overnight at RT or 2 h at 37°C, washed three times with 1 × PBS, and dried before use. Purified cells were plated at 50,000 viable cells per well in 150 μl ABFc-DMEM in a precoated 96-well plate or 8-well chamber slide. Cells adhered to the plate or slide by centrifuging at 300 × g, 5 min, 4°C. A 50-μl single-cell suspension of GFP-*M. tuberculosis* Erdman in ABFc-DMEM, calibrated to deliver *M. tuberculosis* at a multiplicity of infection (MOI) of 5:1, was then added to the wells.

For CD11b⁺ cells, samples were infected in duplicate. The infection proceeded for 2 h at 37°C, 5% CO₂ (30 min of shaking followed by 1.5 h of static incubation). After the 2-h infection, cells were washed three times with ABFc-DMEM and incubated under static conditions in ABFc-DMEM until the indicated time point. For CFU enumeration, cells were centrifuged for 300 × g, 5 min, 4°C, and washed three times with ABFc-DMEM; liquid was removed after the final wash. Cold distilled water (50 μl) containing 500 μg/ml DNase I (Sigma) was added and incubated for 10 min at RT with periodic agitation. 100 μl of OADC-supplemented 7H9 (Difco) medium and 60 μl of 0.25% sodium dodecyl sulfate (Fisher) in 1 × PBS were added and cells incubated for 10 min at RT with periodic agitation. A volume of 75 μl 20% bovine serum albumin (BSA) (Alfa Aesar) in 1 × PBS was added, and wells were mixed by pipetting vigorously several times. Resulting solutions were serially diluted, plated, and incubated as described above. Average CFU numbers are expressed as number of CFU/ml.

For neutrophils, samples were infected in triplicate. The infection proceeded for 30 min at 37°C, 5% CO₂ with constant shaking. After the 30-min infection, cells were washed three times with ABFc-DMEM and incubated under static conditions in ABFc-DMEM until the indicated time point. For CFU enumeration, cells were centrifuged at 300 × g, 5 min, 4°C and washed three times with ABFc-DMEM; liquid was removed after the final wash, and 100 μl 0.1% Triton X-100 (Fisher) in 1 × PBS was added and cells incubated at RT for 15 min with periodic agitation; 100 μl OADC-supplemented 7H9 medium was added, and wells were mixed by pipetting vigorously several times. Resulting solutions were serially diluted, plated, and incubated as described above. Average CFU numbers are expressed as CFU/ml and as the fold change of number of CFU at 2 h versus 30 min (calculated as 2 h divided by 30 min) among samples that originated from the same mouse. For microscopy studies, cells in 8-well chamber slides were washed three times in ABFc-DMEM following the 30-min infection and then fixed in 4% PFA for 15 min prior to ABSL3 removal and further processing.

ICC of in vitro infections. Fixed cells on chamber slides were washed three times with 1 × PBS and stored at 4°C in the dark until staining. Cells were permeabilized by incubating in 0.5% Triton X-100 for 1 min at RT and washed three times with 1 × PBS, 1 min per wash. Blocking buffer (1 × PBS with 10% normal donkey serum [Jackson ImmunoResearch Laboratories], 10 mg/ml BSA, and 0.1% Triton X-100) was added and cells incubated for 30 min at 37°C in a humid chamber. Primary antibodies goat anti-human/mouse myeloperoxidase (MPO) (1:100; AF3667; R&D) and rabbit anti-mouse histone H3 (citruilline R2 + R8 + R17) (1:200; ab5103; Abcam), diluted in blocking buffer, were added and incubated for 1 h at 37°C in a humid chamber. Chamber slides were washed three times with 1 × PBS, 1 min per wash. Secondary antibodies donkey anti-goat IgG Alexa Fluor 647 (1:10,000; A21447; ThermoFisher Scientific) and donkey anti-rabbit IgG Alexa Fluor 568 (1:1,000; A10042; ThermoFisher Scientific), diluted in

blocking buffer, were added and cells incubated for 1 h at 37°C in a humid chamber. Cells were washed as before with three 1-min washes. Chamber slides were then incubated in 4',6-diamidino-2-phenylindole dihydrochloride (DAPI) (1:5,000; ThermoFisher Scientific) in 1 × PBS for 5 min and washed three times in 1 × PBS for 5 min with constant shaking. Chamber slides were mounted with coverslips using Prolong diamond antifade mountant (ThermoFisher Scientific) and dried for at least 24 h prior to imaging. Chamber slides were analyzed using a Zeiss LSM 800 confocal microscope. Nineteen to 22 GFP-*M. tuberculosis* (488 nm) events were counted per well. Histone H3 (citrulline R2 + R8 + R17) and DAPI-smear colocalizations were used to mark neutrophil extracellular traps (NETs), and MPO and circular DAPI were used to mark intact neutrophils. In a single-blinded manner, the locations of GFP-*M. tuberculosis* events were visually assayed as *M. tuberculosis* colocalized with an intact neutrophil or *M. tuberculosis* colocalized with a neutrophil NET. Free *M. tuberculosis* (outside cells or NETS) was also determined, and no differences were observed between groups. Data are presented as percentage of total GFP-*M. tuberculosis* events.

Neutrophil depletion. Anti-mouse Ly6G (300 µg; clone IA8; BP0075-1; BioXCell) or its isotype control rat IgG2a (clone 2A3; BP0089; BioXCell) in 1 × PBS was administered via the i.p. route to LPS/saline mice. Antibody injections began the same day as LPS/saline injections and continued every 48 h. CFU numbers were assessed at 7 days of infection. Single-cell suspensions were isolated at day 0 (uninfected) and analyzed by flow cytometry to assess depletion efficiency. Intracellular Ly6G was used in place of surface Ly6G to account for potential surface antigen masking by the depletion antibody (70). After 2% PFA fixation, intracellular Ly6G was stained in the intracellular staining permeabilization wash buffer (BioLegend) using the manufacturer's protocol. Ly6G antibodies (Ly6G, PE; clone 1A8; BD Pharmingen) used for intracellular staining were diluted half of what was typically used for surface staining.

Statistical analysis. Data analyses, graphing, and statistical analyses were performed using GraphPad Prism 8 and 9 software. Unpaired, two-tailed Student's *t* test was used for two-group comparisons. Statistical significance is reported with asterisks: *, $P < 0.05$; **, $P < 0.01$; ***, $P < 0.001$; ****, $P < 0.0001$. The Grubbs' test was used to identify outlying data points. Data are presented as individual data points and means ± standard errors of the means (SEM).

SUPPLEMENTAL MATERIAL

Supplemental material is available online only.

SUPPLEMENTAL FILE 1, PDF file, 0.7 MB.

ACKNOWLEDGMENTS

We acknowledge Cynthia Canan for her role in project conceptualization and the Texas Biomedical Research Institute Biology Core for their assistance with data collection for flow cytometry and Luminex assays.

Research reported in this publication was supported by the National Institute On Aging of the National Institutes of Health under Award Number P01AG051428, and a Texas Biomedical Research Institute Douglass Foundation Graduate Fellowship. The content is solely the responsibility of the authors and does not necessarily represent the official views of the National Institutes of Health.

T.J.P. and J.T. designed the experiments. T.J.P. and J.M.S. performed the experiments. P.A.P. assisted with mouse procedures. T.J.P. collected and analyzed data and wrote the paper. J.T., J.B.T., and L.S.S. provided critical review of the paper. All authors read and approved the final manuscript.

We declare no conflicts of interest.

REFERENCES

1. WHO. 2020. Global tuberculosis report 2020. WHO, Geneva, Switzerland.
2. Sasindran J, Torrelles J. 2011. *Mycobacterium tuberculosis* infection and inflammation: what is beneficial for the host and for the bacterium? *Front Microbiol* 2:2–16. <https://doi.org/10.3389/fmicb.2011.00002>.
3. Denis M. 1994. Interleukin-12 (IL-12) augments cytolytic activity of natural killer cells toward *Mycobacterium tuberculosis*-infected human monocytes. *Cell Immunol* 156:529–536. <https://doi.org/10.1006/cimm.1994.1196>.
4. Bermudez LE, Wu M, Young LS. 1995. Interleukin-12-stimulated natural killer cells can activate human macrophages to inhibit growth of *Mycobacterium avium*. *Infect Immun* 63:4099–4104. <https://doi.org/10.1128/iai.63.10.4099-4104.1995>.
5. Meraviglia S, El Daker S, Dieli F, Martini F, Martino A. 2011. γδ T cells cross-link innate and adaptive immunity in *Mycobacterium tuberculosis* infection. *Clin Dev Immunol* 2011:587315. <https://doi.org/10.1155/2011/587315>.
6. Lockhart E, Green AM, Flynn JL. 2006. IL-17 production is dominated by gamma-delta T cells rather than CD4 T cells during *Mycobacterium tuberculosis* infection. *J Immunol* 177:4662–4669. <https://doi.org/10.4049/jimmunol.177.7.4662>.
7. Samstein M, Schreiber HA, Leiner IM, Susac B, Glickman MS, Pamer EG. 2013. Essential yet limited role for CCR2⁺ inflammatory monocytes during *Mycobacterium tuberculosis*-specific T cell priming. *Elife* 2:e01086. <https://doi.org/10.7554/eLife.01086>.
8. Vesosky B, Rottinghaus EK, Davis C, Turner J. 2009. CD8 T cells in old mice contribute to the innate immune response to *Mycobacterium tuberculosis* via interleukin-12p70-dependent and antigen-independent production of gamma interferon. *Infect Immun* 77:3355–3363. <https://doi.org/10.1128/IAI.00295-09>.
9. Rottinghaus EK, Vesosky B, Turner J. 2009. Interleukin-12 is sufficient to promote antigen-independent interferon-gamma production by CD8 T cells in

- old mice. *Immunology* 128:e679–e690. <https://doi.org/10.1111/j.1365-2567.2009.03061.x>.
10. Vesosky B, Flaherty DK, Turner J. 2006. Th1 cytokines facilitate CD8-T-cell-mediated early resistance to infection with *Mycobacterium tuberculosis* in old mice. *Infect Immun* 74:3314–3324. <https://doi.org/10.1128/IAI.01475-05>.
 11. Vesosky B, Flaherty DK, Rottinghaus EK, Beamer GL, Turner J. 2006. Age dependent increase in early resistance of mice to *Mycobacterium tuberculosis* is associated with an increase in CD8 T cells that are capable of antigen independent IFN-gamma production. *Exp Gerontol* 41:1185–1194. <https://doi.org/10.1016/j.exger.2006.08.006>.
 12. Havlir DV, Barnes PF. 1999. Tuberculosis in patients with human immunodeficiency virus infection. *N Engl J Med* 340:367–373. <https://doi.org/10.1056/NEJM199902043400507>.
 13. Geldmacher C, Schuetz A, Ngwenyama N, Casazza JP, Sanga E, Saathoff E, Boehme C, Geis S, Maboko L, Singh M, Minja F, Meyerhans A, Koup RA, Hoelscher M. 2008. Early depletion of *Mycobacterium tuberculosis*-specific T helper 1 cell responses after HIV-1 infection. *J Infect Dis* 198:1590–1598. <https://doi.org/10.1086/593017>.
 14. Riou C, Bunjun R, Müller TL, Kiravu A, Ginbot Z, Oni T, Goliath R, Wilkinson RJ, Burgers WA. 2016. Selective reduction of IFN- γ single positive mycobacteria-specific CD4+ T cells in HIV-1 infected individuals with latent tuberculosis infection. *Tuberculosis* 101:25–30. <https://doi.org/10.1016/j.tube.2016.07.018>.
 15. Restrepo BI. 2016. Diabetes and tuberculosis. *Microbiol Spectr* 4:10.1128/microbiolspec.TNMI7-0023-2016. <https://doi.org/10.1128/microbiolspec.TNMI7-0023-2016>.
 16. Tsalamandris S, Antonopoulos AS, Oikonomou E, Papamikroulis GA, Vogiatzi G, Papaioannou S, Deftereos S, Tousoulis D. 2019. The role of inflammation in diabetes: current concepts and future perspectives. *Eur Cardiol* 14:50–59. <https://doi.org/10.15420/ecr.2018.33.1>.
 17. Chakrabarti B, Calverley PM, Davies PD. 2007. Tuberculosis and its incidence, special nature, and relationship with chronic obstructive pulmonary disease. *Int J Chron Obstruct Pulmon Dis* 2:263–272.
 18. Rovina N, Koutsoukou A, Koulouris NG. 2013. Inflammation and immune response in COPD: where do we stand? *Mediators Inflamm* 2013:413735. <https://doi.org/10.1155/2013/413735>.
 19. Lee J, Taneja V, Vassallo R. 2012. Cigarette smoking and inflammation: cellular and molecular mechanisms. *J Dent Res* 91:142–149. <https://doi.org/10.1177/0022034511421200>.
 20. Rajagopalan S. 2001. Tuberculosis and aging: a global health problem. *Clin Infect Dis* 33:1034–1039. <https://doi.org/10.1086/322671>.
 21. Franceschi C, Capri M, Monti D, Giunta S, Olivieri F, Sevini F, Panourgia MP, Invidia L, Celani L, Scurti M, Cevenini E, Castellani GC, Salvioli S. 2007. Inflammaging and anti-inflammaging: a systemic perspective on aging and longevity emerged from studies in humans. *Mech Ageing Dev* 128:92–105. <https://doi.org/10.1016/j.mad.2006.11.016>.
 22. Franceschi C, Campisi J. 2014. Chronic inflammation (inflammaging) and its potential contribution to age-associated diseases. *J Gerontol A Biol Sci Med Sci* 69(Suppl 1):S4–S9. <https://doi.org/10.1093/gerona/glu057>.
 23. Franceschi C, Garagnani P, Vitale G, Capri M, Salvioli S. 2017. Inflammaging and “garb-aging.” *Trends Endocrinol Metab* 28:199–212. <https://doi.org/10.1016/j.tem.2016.09.005>.
 24. Turner J, Orme IM. 2004. The expression of early resistance to an infection with *Mycobacterium tuberculosis* by old mice is dependent on IFN type II (IFN-gamma) but not IFN type I. *Mech Ageing Dev* 125:1–9. <https://doi.org/10.1016/j.mad.2003.09.002>.
 25. Verrall AJ, Schneider M, Alisjahbana B, Apriani L, van Laarhoven A, Koeken VACM, van Dorp S, Diadani E, Utama F, Hannaway RF, Indrati A, Netea MG, Sharples K, Hill PC, Ussher JE, van Crevel R. 2020. Early clearance of *Mycobacterium tuberculosis* is associated with increased innate immune responses. *J Infect Dis* 221:1342–1350. <https://doi.org/10.1093/infdis/jiz147>.
 26. Verrall AJ, Netea MG, Alisjahbana B, Hill PC, van CR. 2014. Early clearance of *Mycobacterium tuberculosis*: a new frontier in prevention. *Immunology* 141:506–513. <https://doi.org/10.1111/imm.12223>.
 27. Harrington AM, Olteanu H, Kroft SH. 2012. A dissection of the CD45/side scatter “blast gate.” *Am J Clin Pathol* 137:800–804. <https://doi.org/10.1309/AJCPN4G1IZPABRLH>.
 28. Hoebe K, Janssen EM, Kim SO, Alexopoulou L, Flavell RA, Han J, Beutler B. 2003. Upregulation of costimulatory molecules induced by lipopolysaccharide and double-stranded RNA occurs by Trif-dependent and Trif-independent pathways. *Nat Immunol* 4:1223–1229. <https://doi.org/10.1038/ni1010>.
 29. Reith W, LeibundGut-Landmann S, Waldburger JM. 2005. Regulation of MHC class II gene expression by the class II transactivator. *Nat Rev Immunol* 5:793–806. <https://doi.org/10.1038/nri1708>.
 30. Ting JP, Trowsdale J. 2002. Genetic control of MHC class II expression. *Cell* 109(Suppl):S21–S33. [https://doi.org/10.1016/s0092-8674\(02\)00696-7](https://doi.org/10.1016/s0092-8674(02)00696-7).
 31. Feng CG, Zheng L, Lenardo MJ, Sher A. 2009. Interferon-inducible immunity-related GTPase Irgm1 regulates IFN gamma-dependent host defense, lymphocyte survival and autophagy. *Autophagy* 5:232–234. <https://doi.org/10.4161/auto.5.2.7445>.
 32. Kamijo R, Harada H, Matsuyama T, Bosland M, Gerecitano J, Shapiro D, Le J, Koh SI, Kimura T, Green SJ, Mak TW, Taniguchi T, Vilcek J. 1994. Requirement for transcription factor IRF-1 in NO synthase induction in macrophages. *Science* 263:1612–1615. <https://doi.org/10.1126/science.7510419>.
 33. Zumla A, Rao M, Parida SK, Keshavjee S, Cassell G, Wallis R, Axelsson-Robertsson R, Doherty M, Andersson J, Maeurer M. 2015. Inflammation and tuberculosis: host-directed therapies. *J Intern Med* 277:373–387. <https://doi.org/10.1111/joim.12256>.
 34. Kumar NP, Fukutani KF, Shruthi BS, Alves T, Silveira-Mattos PS, Rocha MS, West K, Natarajan M, Viswanathan V, Babu S, Andrade BB, Kornfeld H. 2019. Persistent inflammation during anti-tuberculosis treatment with diabetes comorbidity. *Elife* 8:e46477. <https://doi.org/10.7554/eLife.46477>.
 35. Ndlovu H, Marakalala MJ. 2016. Granulomas and inflammation: host-directed therapies for tuberculosis. *Front Immunol* 7:434. <https://doi.org/10.3389/fimmu.2016.00434>.
 36. Piergallini TJ, Turner J. 2018. Tuberculosis in the elderly: why inflammation matters. *Exp Gerontol* 105:32–39. <https://doi.org/10.1016/j.exger.2017.12.021>.
 37. Fulton SA, Reba SM, Martin TD, Boom WH. 2002. Neutrophil-mediated mycobacteriocidal immunity in the lung during *Mycobacterium bovis* BCG infection in C57BL/6 mice. *Infect Immun* 70:5322–5327. <https://doi.org/10.1128/IAI.70.9.5322-5327.2002>.
 38. Sugawara I, Udagawa T, Yamada H. 2004. Rat neutrophils prevent the development of tuberculosis. *Infect Immun* 72:1804–1806. <https://doi.org/10.1128/IAI.72.3.1804-1806.2004>.
 39. Juskewitch JE, Knudsen BE, Platt JL, Nath KA, Knutson KL, Brunn GJ, Grande JP. 2012. LPS-induced murine systemic inflammation is driven by parenchymal cell activation and exclusively predicted by early MCP-1 plasma levels. *Am J Pathol* 180:32–40. <https://doi.org/10.1016/j.ajpath.2011.10.001>.
 40. Hong J, Yoon D, Nam Y, Seo D, Kim JH, Kim MS, Lee TY, Kim KS, Ko PW, Lee HW, Suk K, Kim SR. 2020. Lipopolysaccharide administration for a mouse model of cerebellar ataxia with neuroinflammation. *Sci Rep* 10:13337. <https://doi.org/10.1038/s41598-020-70390-7>.
 41. Copeland S, Warren HS, Lowry SF, Calvano SE, Remick D, Inflammation and the Host Response to Injury Investigators. 2005. Acute inflammatory response to endotoxin in mice and humans. *Clin Diagn Lab Immunol* 12:60–67. <https://doi.org/10.1128/CDLI.12.1.60-67.2005>.
 42. Raduolovic K, Mak'Anyengo R, Kaya B, Steinert A, Niess JH. 2018. Injections of lipopolysaccharide into mice to mimic entrance of microbial-derived products after intestinal barrier breach. *J Vis Exp*. <https://doi.org/10.3791/57610>.
 43. Meneses G, Rosetti M, Espinosa A, Florentino A, Bautista M, Díaz G, Olvera G, Bárcena B, Fleury A, Adalid-Peralta L, Lamoyi E, Fragoso G, Sciuotto E. 2018. Recovery from an acute systemic and central LPS-inflammation challenge is affected by mouse sex and genetic background. *PLoS One* 13:e0201375. <https://doi.org/10.1371/journal.pone.0201375>.
 44. Park BS, Lee JO. 2013. Recognition of lipopolysaccharide pattern by TLR4 complexes. *Exp Mol Med* 45:e66. <https://doi.org/10.1038/emm.2013.97>.
 45. Pålsson-McDermott EM, O'Neill LA. 2004. Signal transduction by the lipopolysaccharide receptor, Toll-like receptor-4. *Immunology* 113:153–162. <https://doi.org/10.1111/j.1365-2567.2004.01976.x>.
 46. Vaure C, Liu Y. 2014. A comparative review of Toll-like receptor 4 expression and functionality in different animal species. *Front Immunol* 5:316. <https://doi.org/10.3389/fimmu.2014.00316>.
 47. Bohatschek M, Werner A, Raivich G. 2001. Systemic LPS injection leads to granulocyte influx into normal and injured brain: effects of ICAM-1 deficiency. *Exp Neurol* 172:137–152. <https://doi.org/10.1006/exnr.2001.7764>.
 48. Iqbal AJ, Fisher EA, Greaves DR. 2016. Inflammation—a critical appreciation of the role of myeloid cells. *Microbiol Spectr* 4:10.1128/microbiolspec.MCHD-0027-2016. <https://doi.org/10.1128/microbiolspec.MCHD-0027-2016>.
 49. Canan CH, Gokhale NS, Carruthers B, Lafuse WP, Schlesinger LS, Torrelles JB, Turner J. 2014. Characterization of lung inflammation and its impact on macrophage function in aging. *J Leukoc Biol* 96:473–480. <https://doi.org/10.1189/jlb.A0214-093RR>.
 50. Moliva JI, Rajaram MV, Sidiki S, Sasindran SJ, Guirado E, Pan XJ, Wang SH, Ross P, Jr, Lafuse WP, Schlesinger LS, Turner J, Torrelles JB. 2014. Molecular composition of the alveolar lining fluid in the aging lung. *Age* 36:9633. <https://doi.org/10.1007/s11357-014-9633-4>.

51. Moliva JI, Duncan MA, Olmo-Fontánez A, Akhter A, Arnett E, Scordo JM, Ault R, Sasindran SJ, Azad AK, Montoya MJ, Reinhold-Larsson N, Rajaram MVS, Merritt RE, Lafuse WP, Zhang L, Wang SH, Beamer G, Wang Y, Proud K, Maselli DJ, Peters J, Weintraub ST, Turner J, Schlesinger LS, Torrelles JB. 2019. The lung mucosa environment in the elderly increases host susceptibility to *Mycobacterium tuberculosis* infection. *J Infect Dis* 220:514–523. <https://doi.org/10.1093/infdis/jiz138>.
52. Turner J, Frank AA, Orme IM. 2002. Old mice express a transient early resistance to pulmonary tuberculosis that is mediated by CD8 T cells. *Infect Immun* 70:4628–4637. <https://doi.org/10.1128/IAI.70.8.4628-4637.2002>.
53. Cooper AM, Callahan JE, Griffin JP, Roberts AD, Orme IM. 1995. Old mice are able to control low-dose aerogenic infections with *Mycobacterium tuberculosis*. *Infect Immun* 63:3259–3265. <https://doi.org/10.1128/iai.63.9.3259-3265.1995>.
54. Mirza N, Pollock K, Hoelzinger DB, Dominguez AL, Lustgarten J. 2011. Comparative kinetic analyses of gene profiles of naïve CD4⁺ and CD8⁺ T cells from young and old animals reveal novel age-related alterations. *Aging Cell* 10:853–867. <https://doi.org/10.1111/j.1474-9726.2011.00730.x>.
55. Lowery EM, Brubaker AL, Kuhlmann E, Kovacs EJ. 2013. The aging lung. *Clin Interv Aging* 8:1489–1496. <https://doi.org/10.2147/CIA.S51152>.
56. Vesosky B, Turner J. 2005. The influence of age on immunity to infection with *Mycobacterium tuberculosis*. *Immunol Rev* 205:229–243. <https://doi.org/10.1111/j.0105-2896.2005.00257.x>.
57. Hilda JN, Das S, Tripathy SP, Hanna LE. 2020. Role of neutrophils in tuberculosis: a bird's eye view. *Innate Immun* 26:240–247. <https://doi.org/10.1177/1753425919881176>.
58. Reiley WW, Calayag MD, Wittmer ST, Huntington JL, Pearl JE, Fountain JJ, Martino CA, Roberts AD, Cooper AM, Winslow GM, Woodland DL. 2008. ESAT-6-specific CD4 T cell responses to aerosol *Mycobacterium tuberculosis* infection are initiated in the mediastinal lymph nodes. *Proc Natl Acad Sci U S A* 105:10961–10966. <https://doi.org/10.1073/pnas.0801496105>.
59. Chackerian AA, Alt JM, Perera TV, Dascher CC, Behar SM. 2002. Dissemination of *Mycobacterium tuberculosis* is influenced by host factors and precedes the initiation of T-cell immunity. *Infect Immun* 70:4501–4509. <https://doi.org/10.1128/IAI.70.8.4501-4509.2002>.
60. Myers AJ, Marino S, Kirschner DE, Flynn JL. 2013. Inoculation dose of *Mycobacterium tuberculosis* does not influence priming of T cell responses in lymph nodes. *J Immunol* 190:4707–4716. <https://doi.org/10.4049/jimmunol.1203465>.
61. Plumlee CR, Duffy FJ, Gern BH, Delahaye JL, Cohen SB, Stoltzfus CR, Rustad TR, Hansen SG, Axthelm MK, Picker LJ, Aitchison JD, Sherman DR, Ganusov VV, Gerner MY, Zak DE, Urdahl KB. 2021. Ultra-low dose aerosol infection of mice with *Mycobacterium tuberculosis* more closely models human tuberculosis. *Cell Host Microbe* 29:68–82.e5. <https://doi.org/10.1016/j.chom.2020.10.003>.
62. Eum SY, Kong JH, Hong MS, Lee YJ, Kim JH, Hwang SH, Cho SN, Via LE, Barry CE, III. 2010. Neutrophils are the predominant infected phagocytic cells in the airways of patients with active pulmonary TB. *Chest* 137:122–128. <https://doi.org/10.1378/chest.09-0903>.
63. Muefong CN, Sutherland JS. 2020. Neutrophils in tuberculosis-associated inflammation and lung pathology. *Front Immunol* 11:962. <https://doi.org/10.3389/fimmu.2020.00962>.
64. Appelberg R, Silva MT. 1989. T cell-dependent chronic neutrophilia during mycobacterial infections. *Clin Exp Immunol* 78:478–483.
65. Lombard R, Doz E, Carreras F, Epardaud M, Le Vern Y, Buzoni-Gatel D, Winter N. 2016. IL-17RA in non-hematopoietic cells controls CXCL-1 and 5 critical to recruit neutrophils to the lung of mycobacteria-infected mice during the adaptive immune response. *PLoS One* 11:e0149455. <https://doi.org/10.1371/journal.pone.0149455>.
66. Lyadova IV. 2017. Neutrophils in tuberculosis: heterogeneity shapes the way? *Mediators Inflamm* 2017:8619307. <https://doi.org/10.1155/2017/8619307>.
67. Moreira-Teixeira L, Stimpson PJ, Stavropoulos E, Hadebe S, Chakravarty P, Ioannou M, Aramburu IV, Herbert E, Priestnall SL, Suarez-Bonnet A, Sousa J, Fonseca KL, Wang Q, Vashakidze S, Rodríguez-Martínez P, Vilaplana C, Saraiva M, Papayannopoulos V, O'Garra A. 2020. Type I IFN exacerbates disease in tuberculosis-susceptible mice by inducing neutrophil-mediated lung inflammation and NETosis. *Nat Commun* 11:5566. <https://doi.org/10.1038/s41467-020-19412-6>.
68. Marzo E, Vilaplana C, Tapia G, Diaz J, Garcia V, Cardona PJ. 2014. Damaging role of neutrophilic infiltration in a mouse model of progressive tuberculosis. *Tuberculosis* 94:55–64. <https://doi.org/10.1016/j.tube.2013.09.004>.
69. Zhang X, Majlessi L, Deriaud E, Leclerc C, Lo-Man R. 2009. Coactivation of Syk kinase and MyD88 adaptor protein pathways by bacteria promotes regulatory properties of neutrophils. *Immunity* 31:761–771. <https://doi.org/10.1016/j.immuni.2009.09.016>.
70. Boivin G, Faget J, Ancey PB, Gkasti A, Mussard J, Engblom C, Pfirschke C, Contat C, Pascual J, Vazquez J, Bendriss-Vermare N, Caux C, Vozenin MC, Pittet MJ, Gunzer M, Meylan E. 2020. Durable and controlled depletion of neutrophils in mice. *Nat Commun* 11:2762. <https://doi.org/10.1038/s41467-020-16596-9>.
71. Stackowicz J, Jönsson F, Reber LL. 2019. Mouse models and tools for the in vivo study of neutrophils. *Front Immunol* 10:3130. <https://doi.org/10.3389/fimmu.2019.03130>.
72. Carr KD, Sieve AN, Indramohan M, Break TJ, Lee S, Berg RE. 2011. Specific depletion reveals a novel role for neutrophil-mediated protection in the liver during *Listeria monocytogenes* infection. *Eur J Immunol* 41:2666–2676. <https://doi.org/10.1002/eji.201041363>.
73. Pollenus E, Malengier-Devliez B, Vandermosten L, Pham TT, Mitera T, Possemiers H, Boon L, Opdenakker G, Matthys P, Van den Steen PE. 2019. Limitations of neutrophil depletion by anti-Ly6G antibodies in two heterogenic immunological models. *Immunol Lett* 212:30–36. <https://doi.org/10.1016/j.imlet.2019.06.006>.
74. Kolaczowska E, Kubes P. 2013. Neutrophil recruitment and function in health and inflammation. *Nat Rev Immunol* 13:159–175. <https://doi.org/10.1038/nri3399>.
75. Rosales C. 2018. Neutrophil: a cell with many roles in inflammation or several cell types? *Front Physiol* 9:113. <https://doi.org/10.3389/fphys.2018.00113>.
76. Gideon HP, Phuah J, Junecko BA, Mattila JT. 2019. Neutrophils express pro- and anti-inflammatory cytokines in granulomas from *Mycobacterium tuberculosis*-infected cynomolgus macaques. *Mucosal Immunol* 12:1370–1381. <https://doi.org/10.1038/s41385-019-0195-8>.
77. Soehnlein O, Steffens S, Hidalgo A, Weber C. 2017. Neutrophils as protagonists and targets in chronic inflammation. *Nat Rev Immunol* 17:248–261. <https://doi.org/10.1038/nri.2017.10>.
78. Hampton MB, Vissers MCM, Winterbourn CC. 1994. A single assay for measuring the rates of phagocytosis and bacterial killing by neutrophils. *J Leukoc Biol* 55:147–152. <https://doi.org/10.1002/jlb.55.2.147>.
79. Ernst JD. 1998. Macrophage receptors for *Mycobacterium tuberculosis*. *Infect Immun* 66:1277–1281. <https://doi.org/10.1128/IAI.66.4.1277-1281.1998>.
80. Neufert C, Pai RK, Noss EH, Berger M, Boom WH, Harding CV. 2001. *Mycobacterium tuberculosis* 19-kDa lipoprotein promotes neutrophil activation. *J Immunol* 167:1542–1549. <https://doi.org/10.4049/jimmunol.167.3.1542>.
81. Faldt J, Dahlgren C, Karlsson A, Ahmed AM, Minnikin DE, Ridell M. 1999. Activation of human neutrophils by mycobacterial phenolic glycolipids. *Clin Exp Immunol* 118:253–260. <https://doi.org/10.1046/j.1365-2249.1999.01040.x>.
82. Scott NR, Swanson RV, Al-Hammadi N, Domingo-Gonzalez R, Rangel-Moreno J, Kriel BA, Bucsan AN, Das S, Ahmed M, Mehra S, Treerat P, Cruz-Lagunas A, Jimenez-Alvarez L, Muñoz-Torrico M, Bobadilla-Lozoya K, Vogl T, Walz G, Du Plessis N, Kaushal D, Scriba TJ, Zúñiga J, Khader SA. 2020. S100A8/A9 regulates CD11b expression and neutrophil recruitment during chronic tuberculosis. *J Clin Invest* 130:3098–3112. <https://doi.org/10.1172/JCI130546>.
83. Sunderkötter C, Nikolic T, Dillon MJ, Van Rooijen N, Stehling M, Drevets DA, Leenen PJ. 2004. Subpopulations of mouse blood monocytes differ in maturation stage and inflammatory response. *J Immunol* 172:4410–4417. <https://doi.org/10.4049/jimmunol.172.7.4410>.
84. Duan M, Steinfurt DP, Smallwood D, Hew M, Chen W, Ernst M, Irving LB, Anderson GP, Hibbs ML. 2016. CD11b immunophenotyping identifies inflammatory profiles in the mouse and human lungs. *Mucosal Immunol* 9:550–563. <https://doi.org/10.1038/mi.2015.84>.
85. Delahaye JL, Gern BH, Cohen SB, Plumlee CR, Shafiani S, Gerner MY, Urdahl KB. 2019. Cutting edge: *Bacillus Calmette-Guérin*-induced T cells shape *Mycobacterium tuberculosis* infection before reducing the bacterial burden. *J Immunol* 203:807–812. <https://doi.org/10.4049/jimmunol.1900108>.
86. Guirado E, Schlesinger LS, Kaplan G. 2013. Macrophages in tuberculosis: friend or foe. *Semin Immunopathol* 35:563–583. <https://doi.org/10.1007/s00281-013-0388-2>.
87. Liu CH, Liu H, Ge B. 2017. Innate immunity in tuberculosis: host defense vs pathogen evasion. *Cell Mol Immunol* 14:963–975. <https://doi.org/10.1038/cmi.2017.88>.
88. Queval CJ, Brosch R, Simeone R. 2017. The macrophage: a disputed fortress in the battle against *Mycobacterium tuberculosis*. *Front Microbiol* 8:2284. <https://doi.org/10.3389/fmicb.2017.02284>.

89. Berrington WR, Hawn TR. 2007. Mycobacterium tuberculosis, macrophages, and the innate immune response: does common variation matter? *Immunol Rev* 219:167–186. <https://doi.org/10.1111/j.1600-065X.2007.00545.x>.
90. Lafuse WP, Rajaram MVS, Wu Q, Moliva JI, Torrelles JB, Turner J, Schlesinger LS. 2019. Identification of an increased alveolar macrophage subpopulation in old mice that displays unique inflammatory characteristics and is permissive to Mycobacterium tuberculosis infection. *J Immunol* 203:2252–2264. <https://doi.org/10.4049/jimmunol.1900495>.
91. Rakotosamimanana N, Richard V, Raharimanga V, Gicquel B, Doherty TM, Zumla A, Rasolofo Razanamparany V. 2015. Biomarkers for risk of developing active tuberculosis in contacts of TB patients: a prospective cohort study. *Eur Respir J* 46:1095–1103. <https://doi.org/10.1183/13993003.00263-2015>.
92. Zelmer A, Stockdale L, Prabowo SA, Cia F, Spink N, Gibb M, Eddaoudi A, Fletcher HA. 2018. High monocyte to lymphocyte ratio is associated with impaired protection after subcutaneous administration of BCG in a mouse model of tuberculosis. *F1000Res* 7:296. <https://doi.org/10.12688/f1000research.14239.2>.
93. Tullius MV, Harth G, Horwitz MA. 2001. High extracellular levels of Mycobacterium tuberculosis glutamine synthetase and superoxide dismutase in actively growing cultures are due to high expression and extracellular stability rather than to a protein-specific export mechanism. *Infect Immun* 69:6348–6363. <https://doi.org/10.1128/IAI.69.10.6348-6363.2001>.
94. Beamer GL, Cyktor J, Flaherty DK, Stromberg PC, Carruthers B, Turner J. 2012. CBA/J mice generate protective immunity to soluble Ag85 but fail to respond efficiently to Ag85 during natural Mycobacterium tuberculosis infection. *Eur J Immunol* 42:870–879. <https://doi.org/10.1002/eji.201142054>.
95. Schlesinger LS, Bellinger-Kawahara CG, Payne NR, Horwitz MA. 1990. Phagocytosis of Mycobacterium tuberculosis is mediated by human monocyte complement receptors and complement component C3. *J Immunol* 144:2771–2780.
96. Beamer GL, Flaherty DK, Vesosky B, Turner J. 2008. Peripheral blood gamma interferon release assays predict lung responses and Mycobacterium tuberculosis disease outcome in mice. *Clin Vaccine Immunol* 15:474–483. <https://doi.org/10.1128/CVI.00408-07>.
97. Abdel-Salam BK, Ebaid H. 2014. Expression of CD11b and CD18 on polymorphonuclear neutrophils stimulated with interleukin-2. *Cent Eur J Immunol* 39:209–215. <https://doi.org/10.5114/ceji.2014.43725>.
98. Fu B, Tian Z, Wei H. 2014. Subsets of human natural killer cells and their regulatory effects. *Immunology* 141:483–489. <https://doi.org/10.1111/imm.12224>.